

IMAGE ZOOMING ALGORITHM BASED ON PARTIAL DIFFERENTIAL EQUATIONS TECHNIQUE

RAN GAO^{1,2}, JIN-PING SONG^{1,2}, AND XUE-CHENG TAI^{3,4}

Abstract. Partial Differential Equations (PDEs) have become an important tool in image processing and analysis. A PDE mode for image zooming is introduced in this paper. This model exploits a higher order nonlinear partial differential equation. The resulted nonlinear equation is solved by an explicit finite difference schemes. Numerical results on real digital images are given to show effectiveness and reliability of the proposed algorithm.

Key Words. image zooming, interpolation, partial differential equations(PDEs)

1. Introduction

Due to the development of modern information technology, image processing is becoming more and more important in our life. Digital zooming is encountered in many real applications such as electronic publishing, image database, digital camera, visible wireless telephone, medical imaging and so on. In order to have better and fine images for users, images often need to be zoomed in and out or reproduced to higher resolution from lower resolution.

One common way for image zooming is interpolating the discrete source image. Interpolation is the first step of two basic re-sampling steps and turns a discrete image into a continuous function, which is necessary for various geometric transform of discrete images. There are two kinds of interpolation methods: linear and non-linear ones. For linear methods, diverse interpolation kernels of finite size have been introduced in the literature. Approximations of the ideal interpolation kernel which is spatially unlimited are essential for these methods, see [5, 9, 17]. The simplest and most popular approximations are related to pixel replication [4], bilinear interpolation [12] and bicubic interpolation methods [7, 6]. They have been routinely implemented in commercial digital image processing softwares. Pixel replication method is a technique of nearest neighbor interpolation [13], which is simple to implement by replicating the original pixels. This method is usually susceptible to the undesirable defect of blocking effects. Bilinear and bicubic interpolation employ first-order spline and second-order spline models, respectively. By doing so, more pleasing outcome is resulted for many real digital images.

A generic zooming algorithm takes as input an RGB picture and provides as output a picture of greater size preserving the information content of the original image as much as possible. Unfortunately, the methods mentioned in the passage above, can preserve the low frequency content of the source image well, but are not equally well to enhance high frequencies in order to produce an image whose visual sharpness matches the quality of the original one. Especially, when the image is zoomed by a large factor, the zoomed image looks very often blocky [14, 15]. In

Received by the editors March 23, 2008 and, in revised form, June 17, 2008.
2000 *Mathematics Subject Classification.* 35R35, 49J40, 60G40.

addition to the problem with sharpness, lower order methods degrade the zoomed image quality, despite the fact that they require less computation effort compared to higher order interpolation methods [2]. One of the basic concepts of the algorithms mentioned above is to interpolate images using the feature of pixels. Determination of pixel feature through these methods needs higher computational complexity, and the result is often disappointing. The method proposed in this paper tries to take into account information about discontinuities or sharp luminance variations.

In recent years, PDEs have achieved great success in the field of image processing [16, 1, 8, 18, 10, 3, 11]. Its basic principle is to use piecewise smooth surfaces to approximate images. Because of the effect of diffusion, the image which has been processed will be quite similar to the original image in edge and other places. Thus, it enables to obtain images not only have good smoothness but also preserve sharpness of the edges. Based on this characteristic, we try to propose a PDE-based interpolation model in this paper. The basic idea of the algorithm is to introduce a fourth-order PDE to smooth the image. Our experiments show that the proposed method is better than bilinear interpolation.

The paper is organized as follows. Our PDE-based model and its numerical realization are formally introduced in Section 2. Section 3 is devoted to numerical experiments, followed by some conclusions in Section 4.

2. PDE-based Image Zooming Algorithm and Its Realization

The PDE model we shall introduce is based on a noise removal algorithm proposed in [15]. In [15], the authors proposed a fourth-order PDE to image denoising, which is to recover an image u from a noisy observation u_0 . This model is referred as the LLT model. For noise removal, one needs to solve the following minimization problem:

$$(1) \min_u E(u), \text{ where } E(u) = \int_{\Omega} (u_{xx}^2 + u_{xy}^2 + u_{yx}^2 + u_{yy}^2)^{\frac{1}{2}} dx dy + \frac{\lambda}{2} \int_{\Omega} |u - u_0|^2 dx dy.$$

Assume the noise level $\sigma^2 = \int_{\Omega} |u - u_0|^2 dx dy$ is approximately known, then one can use a Lagrangian multiplier to solve the above constrained minimization problem. The resulted equation is a fourth order nonlinear partial differential equation. High-order PDEs are known to recover smoother surfaces better. The nonlinear PDE resulted from LLT can also preserve jump rather well. In this work, we try to use this idea for image zooming.

2.1. The PDE-based model. To formulate the problem in the continuous setting, we assume that the low resolution image $u_0(x, y), (x, y) \in \Omega_1$ is given in $\Omega_1 \subset \Omega$ and $\Omega = \Omega_1 \cup \Omega_2$. In the discrete setting, Ω_1 contains the grid points of the low resolution image pixels. From the values of u_0 in Ω_1 , we want to extend them to the whole region Ω .

For this purpose, we shall try to find a function u defined in the whole region to minimize the energy functional:

$$(2) E(u) = \int_{\Omega} (u_{xx}^2 + u_{xy}^2 + u_{yx}^2 + u_{yy}^2)^{\frac{1}{2}} dx dy + \frac{\lambda}{2} \int_{\Omega} |u - u_0|^2 \cdot \chi_{\Omega_1}(u - u_0) dx dy.$$

Above, χ_{Ω_1} is the 'characteristic function' of Ω_1 . The first term in $E(u)$ is a smoothing term and it is used to guarantee that recovered image has smooth level curves. The parameter λ is a positive weighting constant that controls contribution of fidelity term. Minimizing the continuous energy functional $E(u)$ yields a nonlinear fourth-order PDE. Thereby, we obtain a PDE-based interpolation model.

u_{ij}^0	<i>Initial</i>
$D_x^\pm(u_{ij})$	$\pm \frac{1}{\Delta x} [u_{i\pm 1,j} - u_{ij}]$
$D_y^\pm(u_{ij})$	$\pm \frac{1}{\Delta y} [u_{i,j\pm 1} - u_{ij}]$
$D_{xx}(u_{ij})$	$\frac{1}{\Delta x} [D_x^+(u_{ij}) - D_x^+(u_{i-1,j})]$
$D_{xy}^\pm(u_{ij})$	$\pm \frac{1}{\Delta y} [D_x^\pm(u_{i,j\pm 1}) - D_x^\pm(u_{ij})]$
$D_{yx}^\pm(u_{ij})$	$\pm \frac{1}{\Delta y} [D_y^\pm(u_{i\pm 1,j}) - D_y^\pm(u_{ij})]$
$D_{yy}(u_{ij})$	$\frac{1}{\Delta y} [D_y^\pm(u_{i,j}) - D_y^\pm(u_{i,j-1})]$
$ D^2 u_{ij} $	$\sqrt{((D_{xx} u_{ij})^2 + (D_{xy}^+(u_{ij}))^2 + (D_{yx}^+(u_{ij}))^2 + (D_{yy}(u_{ij}))^2 + \epsilon)}$

TABLE 1. Discretizations used in the article

For simplicity, we introduce the notation $|D^2 u| = \int_{\Omega} (u_{xx}^2 + u_{xy}^2 + u_{yx}^2 + u_{yy}^2)^{\frac{1}{2}}$ and write

$$(3) \quad E(u) = \int_{\Omega} |D^2 u| dx dy + \frac{\lambda}{2} \int_{\Omega} |u - u_0|^2 \cdot \chi_{\Omega_1}(u - u_0) dx dy.$$

To find a minimizer for $E(u)$, we see that

$$(4) \quad \frac{\partial E}{\partial u} \cdot v = \int_{\Omega} \left(\frac{\nabla u_x \cdot \nabla v_x + \nabla u_y \cdot \nabla v_y}{|D^2 u|} \right) dx dy + \lambda \int_{\Omega} (u - u_0)v \cdot \chi_{\Omega_1}(u - u_0) dx dy.$$

Using Green's lemma on the first part of (4) we get

$$(5) \quad \begin{aligned} \int_{\Omega} \left(\frac{\nabla u_x \cdot \nabla v_x + \nabla u_y \cdot \nabla v_y}{|D^2 u|} \right) dx dy &= \int_{\partial\Omega} \left[\left(\frac{1}{|D^2 u|} \frac{\partial u_x}{\partial \vec{n}} \right) v_x + \left(\frac{1}{|D^2 u|} \frac{\partial u_y}{\partial \vec{n}} \right) v_y \right] dS \\ &\quad - \int_{\partial\Omega} \left[\nabla \cdot \left(\frac{\nabla u_x}{|D^2 u|} \right) \vec{n}_1 v + \nabla \cdot \left(\frac{\nabla u_y}{|D^2 u|} \right) \vec{n}_2 v \right] dS \\ &\quad + \int_{\Omega} \left[\left(\nabla \cdot \left(\frac{\nabla u_x}{|D^2 u|} \right) \right)_x v + \left(\nabla \cdot \left(\frac{\nabla u_y}{|D^2 u|} \right) \right)_y v \right] dx dy. \end{aligned}$$

Where dS denotes the surface measure on $\partial\Omega$. Here and later, the unit normal vector on $\partial\Omega$ is denoted by $\vec{n} = (n_1, n_2)$. From this, we see that a minimum for (4) satisfies

$$(6) \quad \left(\frac{u_{xx}}{|D^2 u|} \right)_{xx} + \left(\frac{u_{xy}}{|D^2 u|} \right)_{yx} + \left(\frac{u_{yx}}{|D^2 u|} \right)_{xy} + \left(\frac{u_{yy}}{|D^2 u|} \right)_{yy} + \lambda(u - u_0) \cdot \chi_{\Omega_1}(u - u_0) = 0.$$

According to the Euler-Lagrange variational principle, the minimizer of $E(u)$ can be interpreted as the steady state solution of the nonlinear diffusion process

$$(7) \quad u_t = - \left[\left(\frac{u_{xx}}{|D^2 u|} \right)_{xx} + \left(\frac{u_{xy}}{|D^2 u|} \right)_{yx} + \left(\frac{u_{yx}}{|D^2 u|} \right)_{xy} + \left(\frac{u_{yy}}{|D^2 u|} \right)_{yy} + \lambda(u - u_0) \cdot \chi_{\Omega_1}(u - u_0) \right].$$

Moreover, the variational equality (4) implies the following boundary conditions

$$(8) \quad \left. \begin{aligned} u_{xx} + u_{yy} &= 0 \\ \left(\frac{u_{xx}}{|D^2 u|} \right)_x + \left(\frac{u_{xy}}{|D^2 u|} \right)_y &= 0 \end{aligned} \right\} \text{ on } \partial\Omega \text{ where } n \text{ is orthogonal to the } y - \text{axe,}$$

$$(9) \quad \left. \begin{aligned} u_{xy} + u_{yx} &= 0 \\ \left(\frac{u_{yx}}{|D^2 u|} \right)_x + \left(\frac{u_{yy}}{|D^2 u|} \right)_y &= 0 \end{aligned} \right\} \text{ on } \partial\Omega \text{ where } n \text{ is orthogonal to the } x - \text{axe.}$$

Combining (7) and (8)-(9), we get the PDE-based interpolation model.

2.2. Implementation details. To discretize equation (7), finite differences approximations will be introduced. Let $\Delta x, \Delta y$ be the mesh sizes for the x, y variables, while Δt be the time step. We denote by u^n the approximations for $u(x, y, n\Delta t)$. The approximations we have used in our scheme is outlined in Table 1.

Given the low resolution image u_0 of size $M \times N$, we want to get a zoomed image of size $(M \cdot k) \times (M \cdot k)$. Here, M, N, k are positive integers. First, we use bilinear interpolation to extend u_0 to all the $(M \cdot k) \times (N \cdot k)$ mesh grid points and use this as the initial value u^0 . Then update the solution by

$$\begin{aligned}
 u^{n+1} &= u^n \\
 & - \Delta t \left[D_{xx} \left(\frac{D_{xx} u^n}{|D^2 u^n|} \right) + D_{yx}^- \left(\frac{D_{xy}^+ u^n}{|D^2 u^n|} \right) + D_{xy}^+ \left(\frac{D_{yx}^- u^n}{|D^2 u^n|} \right) + D_{yy} \left(\frac{D_{yy} u^n}{|D^2 u^n|} \right) \right] \\
 (10) \quad & - \Delta t \lambda (u^n - u_0) \cdot \chi_{\Omega_1} (u^n - u_0).
 \end{aligned}$$

When u^n has reached a steady state, it is taken as the zoomed image. When evaluating the finite differences for (7), the boundary conditions (8) and (9) are needed. Implementation of these conditions shall be done in the standard way.

3. Numerical Experiments

Several experiments with the proposed algorithm have been performed. We present a few of them in this section. First, we use a image named 'Circel' to compare our algorithm with the bilinear interpolation, see Figure 1. In addition, we shall also present our experimental results for images such as 'Elaine', 'Lena', 'Portion of Elaine', 'Portion of Peppers' and two color images 'Lily' and "Seaside", see Figures 1-4.

It's known that with large Δt , the iterations will converge faster. But if they are too large, the scheme will be unstable and will not converge to a steady state. It is then necessary to choose a reasonable smaller time step. It is usual to choose Δt by trial and error based on our experience. For most experiments, we always use fixed time step $\Delta t \approx 10^{-3}$. We chose $\Delta x = \Delta y = 0.15$, and the parameter λ is set equal to 500. The value of ε is set equal to 10^{-11} in all the tests.

We usually observe the quality of a zoomed image by visual examinations. However, to show numerical evidence of the our algorithm, peak signal-to-noise ratio (PSNR) is also used here to measure the image quality. The PSNR is defined as

$$PSNR = 10 \lg \frac{255^2}{MSE} dB$$

Where

$$MSE = \frac{\sum_{i,j}^{M,N} (I(i, j) - J(i, j))^2}{\sum_{i,j}^{M,N} (I(i, j))^2}$$

Here, (M, N) is the size of original high-resolution image, I, J are the original and zoomed images respectively. In order to measure the PSNR value and the MSE value, the original image is reduced to small one by sampling. Then it can be zoom back to its original size using our zooming method. We compare the zoomed image with the original image.

Many image zooming techniques suffers from the so called "checkerboard effect". In Figure 1, the binary image 'Circle' is zoomed by the bilinear interpolation, see Fig.1. In Fig.1.(a), a down-sampled image of size 32×31 from the original image

Fig.1.(b) of size 128×124 is displayed. Fig.1.(c) and Fig.1.(d) show the zoomed images obtained by bilinear interpolation and our algorithm. They have the same size as to the original image in Fig.1.(b). It is clear to see the "checkerboard effect" in the interpolated image in Fig.1.(c). However, our new model does not have this problem. The boundary of the 'Circle' in Fig.1.(d) is smooth and does not have the zigzag effect as that in Fig.1.(c), showing that our algorithm preserves the smoothness of the brim of 'Circle'.

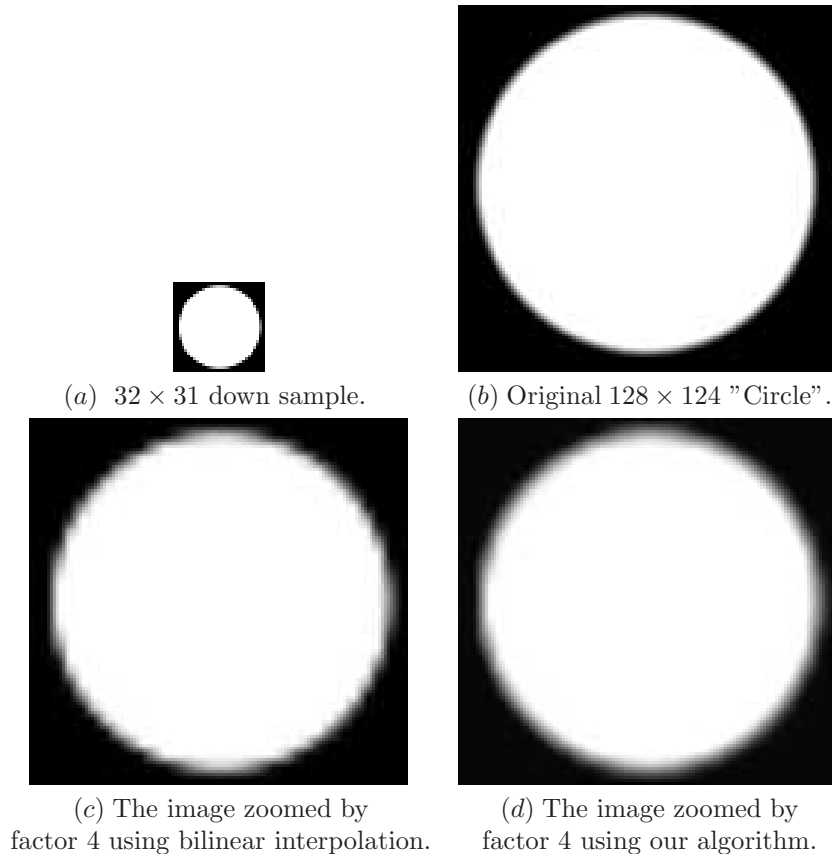


FIGURE 1. Binary image zoomed by bilinear and our algorithm.

In Fig.2, we test the performances of our algorithm for a gray-scale image. Fig.2.(d) is the zoomed gray-scale 'Elaine' image from the down sampled image by the factor 4 as shown in Fig.2.(a). We can see the quality of our algorithm, although zoomed by large factor, the discontinuities of the image are well preserved and it does not suffer from the checkerboard effect as that in Fig.2.(c).

Furthermore, in order to show the efficiency of our algorithm, we give some other examples in the following. In Fig.3, the results of two gray-scale images are given. Here we use a small portion of the 'Lena' and 'Peppers' images as the test images respectively in Fig.3.(a) and (b). Fig.3.(c) and (d) show the zoomed images by a factor of 6. Compared with the original image, see Fig.3.(c) and (d), the zoomed images faithfully reflected the primitive appearance of the original images, and maintained the edge sharpness and the texture characteristic, showing that our algorithm obtains better visual impression.

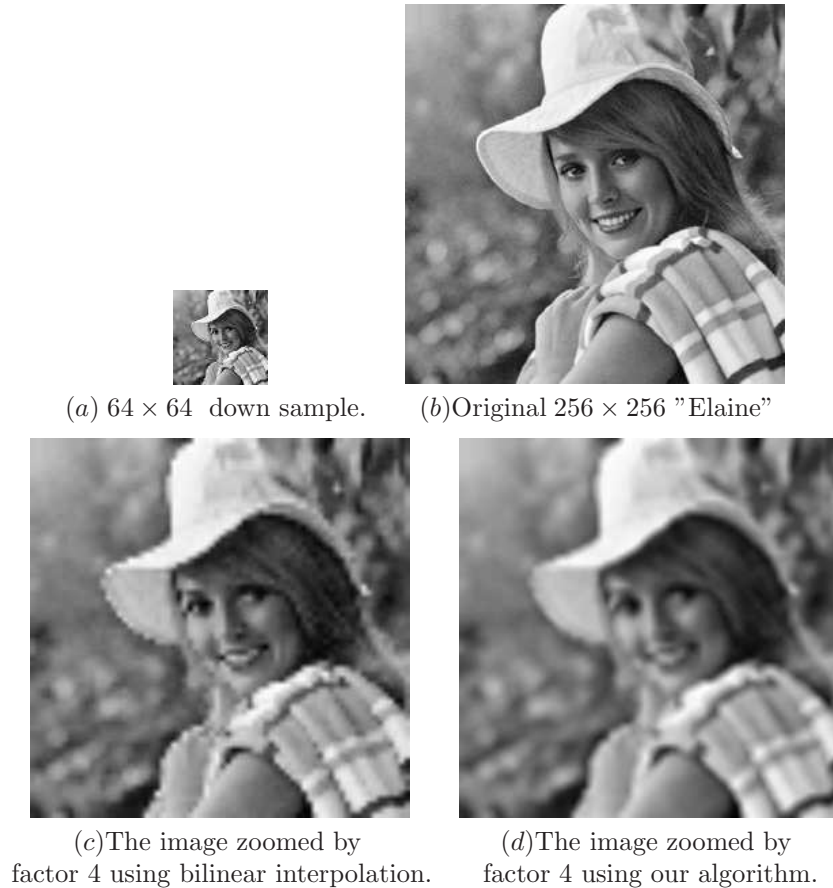


FIGURE 2. Gray-Scale images zoomed by our algorithm and bilinear interpolation.

In order to use the subjective standards to show the efficiency of our algorithm, we give some values of PSNR and MSE in Table 2. In the table, the data is obtained when the original images are zoomed by a factor of 4. As shown in Table 2, our algorithm improves the PSNR and MSE for all cases and all the data are obtained when the energy functional has been stabilized. The improvement of PSNR is great for both the binary and gray-scale images.

Digital color images are more common than gray-scale images. To demonstrate the validity of our algorithm, we have also conducted an experiment on color image zooming. We take the "Lily" image and "Seaside" images of size 100×100 as test examples. The results are shown in Fig.4. By visual inspections of the zoomed images Fig.4.(c) and (d)), we see that the color of the zoomed images are brightly, and the discontinuities are sharp. The image quality of the zoomed image is desirable.

4. Conclusions

In this paper, we proposed an image zooming method based on a nonlinear PDEs. Anisotropic diffusion has been incorporated through the numerical discretization

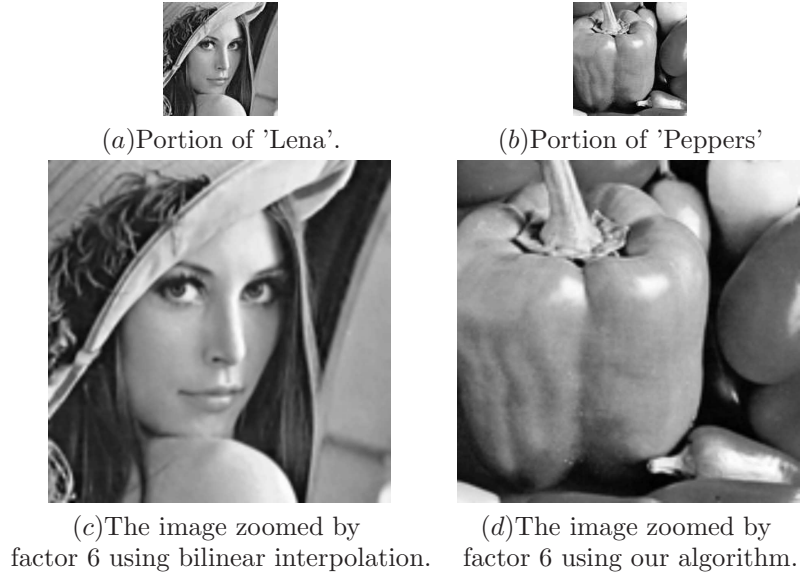


FIGURE 3. The gray-level image zoomed by our algorithm.

<i>image</i>	<i>method</i>	<i>PSNR</i>	<i>MSE</i>
<i>Circle</i>	<i>bilinear</i>	11.9297	$2.5689e - 004$
	<i>our</i>	12.1939	$2.4173e - 004$
<i>Elaine</i>	<i>bilinear</i>	6.1244	$1.8897e - 004$
	<i>our</i>	6.3941	$1.7760e - 004$
<i>Lena</i>	<i>bilinear</i>	13.3496	$2.0249e - 004$
	<i>our</i>	13.4932	$1.9590e - 004$
<i>Peppers</i>	<i>bilinear</i>	9.4164	$5.0980e - 004$
	<i>our</i>	10.5203	$3.9538e - 004$

TABLE 2. PSNR and MSE comparison of the zoomed images using our method and bilinear.

of the model. All the examples indicate that our algorithm is efficient for image zooming and has good subjective quality, both for gray-level and color images.

Acknowledgments

This work is supported by National Natural Science Committee and Chinese Engineering Physics Institute foundation, the National Nature Science Foundation of Henan Province of China.



(a)Portion of 'lily'.



(b)Portion of 'Seaside'.



(c)Zoomed image by our algorithm.



(d)Zoomed image by our algorithm.

FIGURE 4. Color images, zoomed by our algorithm.

References

- [1] T. Chan and J. Shen, Image processing and analysis – Variational, PDE, wavelet, and stochastic methods. Society for Industrial and Applied Mathematics (SIAM), Philadelphia, PA, 2005.
- [2] Chin-Chen Chang, Yung-Chen Chou, Yuan-Hui Yu, Kai-Jung Shih, An image zooming technique based on vector quantization approximation, Image and Vision Computing 23 (2005) 1214-1225.
- [3] J. D. Finley, Commun. Math. Phys. 178, 375-390 (1996).
- [4] R.C. Gonzalez, R.C. Gonzalez, R.E. Woods, Digital Image Processing, Addison-Wesley, Reading MA, 1992.
- [5] R. Gonzalez and R. Woods, Digital Image Processing, 2nd Ed. Upper Saddle River, New Jersey: Prentice-Hall, Inc.,2002.
- [6] H.S. Hou, H.S. Hou, H.C. Andrews, Cubic splines for image interpolation and digital filtering, IEEE Trans. Acoust., Speech, Signal Processing ASSP-26 (6) (1978) 508C517.
- [7] R. Keys, Cubic convolution interpolation for digital image processing, IEEE Trans. Acoust., Speech, Signal Processing ASSP-26 (6) (1978) 508C517.
- [8] R. Kimmel. Numerical geometry of images. Theory, algorithms, and applications. Springer-Verlag, New York, 2004.
- [9] T. Lehmann, C. Gonner, and K. Spitzer, "Survey: Interpolation methods in medical image processing," IEEE Trans. Medical Imaging, vol. 18, no. 11, pp. 1049-1075, 1999.
- [10] M. Lysaker, A. Lundervold, and X.-C. Tai, Noise Removal Using Fourth-Order Partial Differential Equation with Applications to Medical Magnetic Resonance Images in Space and Time," IEEE Trans. Image Processing, vol.12, no. 12, pp. 1579-1590, 2003.
- [11] M. Lysaker, S. Osher, and X.-C. Tai, "Noise Removal Using Smoothed Normal and Surface Fitting", IEEE Trans. Image Processing, vol. 13, no. 10, pp. 1345-1357, 2004.
- [12] E. Maeland , On the comparison of interpolation methods, IEEE Trans. Med. Imag. 7(3)(1988) 213-217.
- [13] J.A Parker, R.V Kenyon, D.E Troxel, Comparison of interpolating methods for image re-sampling, IEEE Trans.Med.Imag.MI-2(1)(1983)31-39.
- [14] E. Polidori, J.L. Dugelay, Zooming using iterated function systems, Fractals 5 (1997) 111-123.

- [15] M.A Pumar, Zooming of terrain imagery using fractal-based interpolation, *Computers Graphics* 20 (1)(1996)171-176.
- [16] X.-C. Tai, K. Lie, T. Chan, and S. Osher. *Image processing based on partial differential equations*. Springer Verlag, Heidelberg, 2007.
- [17] M. Unser, A. Aldroubi, and M. Eden, "Enlargement and reduction of digital images with minimum loss of information," *IEEE Trans. Image Process.*, vol. 4, pp. 247-257, 1995.
- [18] J. Weickert, *Anisotropic diffusion in image processing*. European Consortium for Mathematics in Industry. B. G. Teubner, Stuttgart, 1998.

1. Institute of Mathematics, Henan University, Kaifeng 475004, China., 2. College of Mathematics and Information Science, Henan University, Kaifeng 475004, China.

E-mail: nygr@163.com

1. Institute of Mathematics, Henan University, Kaifeng 475004, China., 2. College of Mathematics and Information Science, Henan University, Kaifeng 475004, China.

E-mail: songjp@henu.edu.cn.

3. Division of Mathematical Sciences, School of Physical and Mathematical Sciences, Nanyang Technological University, Singapore., 4. Department of Mathematics, University of Bergen, N-5008, Bergen, Norway.

E-mail: Tai@mi.uib.no

URL: <http://www.mi.uib.no/~tai/>